Improved Direct Power Control for Grid-Connected Voltage Source Converters

Gui, Yonghao; Kim, Chunghun; Chung, Chung Choo; Guerrero, Josep M.; Guan, Yajuan; Quintero, Juan Carlos Vasquez

Published in:
I E E E Transactions on Industrial Electronics

DOI (link to publication from Publisher):
10.1109/TIE.2018.2801835

Publication date:
2018

Document Version
Accepted author manuscript, peer reviewed version

Improved Direct Power Control for Grid-Connected Voltage Source Converters

Yonghao Gui, *Member, IEEE*, Chunghun Kim, *Member, IEEE*,, Chung Choo Chung, *Member, IEEE*, Josep M. Guerrero, *Fellow, IEEE*, Yajuan Guan, *Member, IEEE*, and Juan C. Vasquez, *Senior Member, IEEE*

***Abstract*—A novel grid voltage modulated direct power control (GVM-DPC) strategy for a grid-connected voltage source converter is proposed to control the instantaneous active and reactive powers directly. The GVM-DPC method consists of a nonlinear GVM controller, a conventional controller (feedforward and PI feedback), and nonlinear damping. The proposed control strategy shows a relationship between DPC and voltage-oriented control methods designed in d-q frame. The main advantage is that the proposed method makes the system be a linear time-invariant system, which enables us to apply various control methods easily. The GVM-DPC guarantees not only the convergence rate but also the steady-state performance of the system. Moreover, it is ensured that the closed-loop system is exponentially stable. Finally, simulation and experimental results using a 2.2-kVA VSC are provided to validate the tracking performance and robustness of the proposed control architecture. In addition, the total harmonic distortion of the current is 1.9% which is much less than the requirement for grid operation.**

***Index Terms*—Direct power control, DC-AC power converters, linear time-invariant system, exponentially stable.**

I. Introduction

RECENTLY, control of power converters is a hot issue because of the rapid development of smart grid, flexible AC transmission systems, high-voltage DC systems, and renewable energy sources such as wind and solar power [1]–[8]. It is essential to use power converter systems for energy sustainability, which aims to generate electricity from renewable sources and use it efficiently [9]. Consequently, power converter systems are increasingly utilized in various applications (*e.g.* power conditioning, compensation, and power filtering, etc.) [10]–[13].

One of the key devices of power converters is grid-connected voltage source converter (VSC) which supports the several roles for grid operation. The conventional control of grid-connected VSC is designed in a synchronous rotating reference frame and a decoupled proportional integral (PI) control is applied for separately controlling *d*–*q* axes currents, i.e. controlling active and reactive powers separately [14]. An enhanced vector control method with additional PI controllers is proposed to handle the undesirable current oscillations in the double synchronous reference frame [15]. The main disadvantages of the conventional methods are a highly sensitive performance to the completeness of the current decoupling, the accuracy of tuning of the PI gains, and the grid voltage conditions, etc.

To control instantaneous active and reactive powers directly without using any inner-loop current regulators, various direct power control (DPC) methods have been proposed for VSCs [16]–[24]. A look-up-table (LUT)-DPC with hysteresis is proposed by selecting the converter switching signals directly from a predefined optimal switching table [16]. However, the switching frequency of the LUT-DPC method changes according to the switching state. Besides, an unexpected broadband harmonic spectrum range is generated, that means it is not easy to design a line filter. To solve such disadvantage, some DPC strategies have been proposed to achieve a constant switching frequency [17]–[19]. For robust control, a DPC with sliding mode control (SMC) method is proposed in the stationary reference frame [20], [21]. The SMC-DPC brings an exponential convergence of the tracking error on the manifolds which are defined as tracking errors of active and reactive powers and their integrals. Although the SMC-DPC obtains a faster settling response than that of the PI controller and more robustness against parameter uncertainty than that of the LUT-DPC, the convergence to its equilibrium point is not guaranteed. To overcome this problem, port-controlled Hamiltonian (PCH) DPC is designed based on the system's intrinsic dissipative nature [24], but there are still power ripples in both active and reactive powers.

Recently, another popular control strategy of DPC, model predictive control (MPC), has been applied to power converters in order to handle the multivariable case, system constraints, and nonlinearities in an intuitive way [25]–[28]. MPC-DPC selects voltage vector sequence and calculates duty cycles in every sampling period, One of the advantages is that it provides a constant switching frequency [29]–[31]. Conventionally, MPC-DPC strategy performs a good closed-loop behavior. However, an incorrect voltage sequence selection could affect its performance [32]. To solve this problem, an optimal voltage sequence is redesigned in [33], but it

This research was supported by the Korea Electric Power Corporation. (grant number: R17XA05-56).

Y. Gui was with the Dept. of Electrical Engineering, Hanyang University, Seoul, Korea and is currently with the Dept. of Energy Technology, Aalborg University, Aalborg 9220, Denmark. (e-mail: yog@et.aau.dk).

C. Kim and C. C. Chung are with the Dept. of Electrical Engineering, Hanyang University, Seoul 04763, Korea. (e-mail: freidee@hanyang.ac.kr; cchung@hanyang.ac.kr).

J. M. Guerrero, Y. Guan, and J. C. Vasquez are with the Dept. of Energy Technology, Aalborg University, Aalborg 9220, Denmark (e-mail: joz@et.aau.dk; ygu@et.aau.dk; juq@et.aau.dk).

incurs additional computational burden. To overcome such computational issue, a new strategy is proposed to adopt fixed voltage vectors without using the angular information of the grid-voltage vector or the virtual-flux vector [34]. Moreover, optimal switching sequence DPC is investigated without using grid voltage sector information or lookup tables, but it takes advantage of the discrete nature of the power converter [35]. In [36], the modified MPC-DPC is proposed for a high-power grid-connected neutral-point-clamped converter with a lower switching frequency.

The motivation of this manuscript is to design a robust but simple control law for not only the convergence rate of the instantaneous active and reactive powers but also the steady-state performance of VSC, especially reduction of power ripples and total harmonics distortion (THD) of the output current. The proposed grid voltage modulated direct power control (GVM-DPC) method consists of a nonlinear GVM controller, a tracking controller, and additional feedback. The nonlinear GVM control generates two new control inputs that can present the original system in d–q frame without using a phase-locked loop. Another advantage is that the GVM-DPC converts the original system into a linear time-invariant (LTI) MIMO system. Thus, various control methods designed in d–q frame can be applied to the new LTI MIMO system. In this paper, the tracking controller consists of feedforward and PI feedback, which are used to control two separate second-order error dynamics of active and reactive powers. It is guaranteed that the closed-loop system with the proposed method is exponentially stable in the whole operating range. Moreover, the damping ratio and the convergence rate of the active and reactive powers could be designed by selecting the controller gains.

Although the GVM-DPC is firstly introduced in [37], in this paper, a damping feedback controller is additionally designed to improve robust property against the model and parameter uncertainties without losing stability. The simulation results are compared with the SMC-DPC and PCH-DPC which has a better performance than SMC-DPC. Moreover, the proposed method is experimentally tested in order to evaluate the effectiveness rather than using a hardware-in-the-loop system.

The rest of the paper is organized as follows. In Section II, the system modeling and the control design of the GVM-DPC are presented. Section III shows the simulation results using MATLAB/Simulink and PLECS blockset. Section IV presents the experimental results of a 2.2-kW-inverter system. Finally, the conclusions are given in Section V.

II. Grid Voltage Modulated Direct Power Control

In this Section, firstly, a DPC modeling of VSC is briefly introduced. For the VSC system, the GVM-DPC is designed to make it be an LTI MIMO system, then a feedforward and a feedback controller are designed to make the error dynamics stable. Finally, an additional feedback controller is designed to improve the robust property of the model and parameter uncertainties without losing stability.

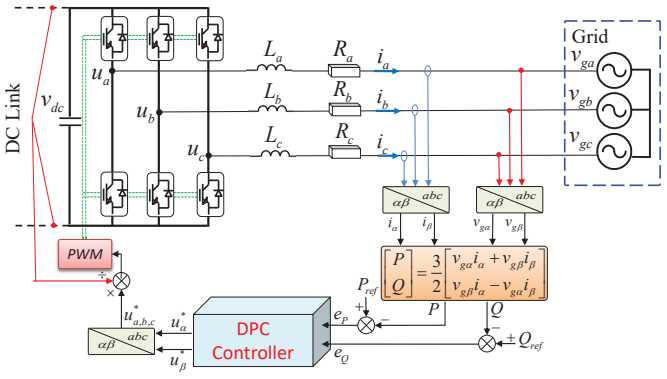

Fig. 1. DPC for a grid-connected two level VSC with an L filter.

A. DPC Modeling of VSC

Fig. 1 shows a simplified circuit of a two-level VSC connected to the grid with an L-filter. Based on a balanced grid voltage condition, the relationships among the VSC output voltages, the grid voltages, and the output currents in the stationary reference frame can be expressed as follows [20], [38]:

$$\begin{aligned} u_\alpha &= Ri_\alpha + L\frac{di_\alpha}{dt} + v_{g\alpha}, \\ u_\beta &= Ri_\beta + L\frac{di_\beta}{dt} + v_{g\beta}, \end{aligned} \tag{1}$$

where u_α and u_β indicate the VSC output voltages, i_α and i_β indicate the output currents, $v_{g\alpha}$ and $v_{g\beta}$ indicate the grid voltages in α-β frame, and L and R are the filter inductance and resistance, respectively. The instantaneous active and reactive powers in the stationary reference frame can be defined as follows:

$$\begin{aligned} P &= \frac{3}{2}(v_{g\alpha}i_\alpha + v_{g\beta}i_\beta), \\ Q &= \frac{3}{2}(v_{g\beta}i_\alpha - v_{g\alpha}i_\beta), \end{aligned} \tag{2}$$

where P and Q are the instantaneous active and reactive powers, respectively. By differentiating (2) with respect to time, the instantaneous active and reactive powers variations can be expressed regarding grid voltage and output current variations as follows:

$$\begin{aligned} \frac{dP}{dt} &= \frac{3}{2}\left(i_\alpha\frac{dv_{g\alpha}}{dt} + v_{g\alpha}\frac{di_\alpha}{dt} + i_\beta\frac{dv_{g\beta}}{dt} + v_{g\beta}\frac{di_\beta}{dt}\right), \\ \frac{dQ}{dt} &= \frac{3}{2}\left(i_\alpha\frac{dv_{g\beta}}{dt} + v_{g\beta}\frac{di_\alpha}{dt} - i_\beta\frac{dv_{g\alpha}}{dt} - v_{g\alpha}\frac{di_\beta}{dt}\right). \end{aligned} \tag{3}$$

If we consider a nondistorted grid, the following relationship could be obtained.

$$\begin{aligned} v_{g\alpha} &= V_g\cos(\omega t), \\ v_{g\beta} &= V_g\sin(\omega t), \end{aligned} \tag{4}$$

where ω is the angular frequency of the grid voltage and $\omega = 2\pi f$, and f is the frequency of the grid voltage. V_g is the magnitude of the grid voltage. Differentiating (4) with

respect to time, the instantaneous grid voltage variations can be expressed as follows:

$$\begin{aligned}\frac{dv_{g\alpha}}{dt} &= -\omega V_g \sin(\omega t) = -\omega v_{g\beta},\\ \frac{dv_{g\beta}}{dt} &= \omega V_g \cos(\omega t) = \omega v_{g\alpha}.\end{aligned} \tag{5}$$

Substituting (1) and (5) into (3), the state-space model of the active and reactive powers is obtained as follows:

$$\begin{aligned}\frac{dP}{dt} &= -\frac{R}{L}P - \omega Q + \frac{3}{2L}(v_{g\alpha}u_\alpha + v_{g\beta}u_\beta - V_g^2),\\ \frac{dQ}{dt} &= \omega P - \frac{R}{L}Q + \frac{3}{2L}(v_{g\beta}u_\alpha - v_{g\alpha}u_\beta).\end{aligned} \tag{6}$$

B. Grid Voltage Modulated Direct Power Control

As represented in (6), the dynamics of instantaneous active and reactive powers in α–β frame is a time-varying MIMO system, and both control inputs are coupled in both states P and Q. Consequently, our main idea is to decouple the outputs from the two inputs. Define the GVM control inputs such as

$$\begin{aligned}u_P &:= v_{g\alpha}u_\alpha + v_{g\beta}u_\beta,\\ u_Q &:= -v_{g\beta}u_\alpha + v_{g\alpha}u_\beta.\end{aligned} \tag{7}$$

Based on the grid voltage (4), the GVM inputs can be represented in d–q frame as follows:

$$\begin{bmatrix}u_P\\ u_Q\end{bmatrix} = V_g \begin{bmatrix}\cos(\omega t) & \sin(\omega t)\\ -\sin(\omega t) & \cos(\omega t)\end{bmatrix}\begin{bmatrix}u_\alpha\\ u_\beta\end{bmatrix} = V_g \begin{bmatrix}u_d\\ u_q\end{bmatrix}, \tag{8}$$

where u_d and u_q are the converter voltages in d–q frame. The proposed method does not use the PLL, but the system is presented in d–q frame. Consequently, $f(x,u)$ can be rewritten as follows:

$$\begin{aligned}\frac{dP}{dt} &= -\frac{R}{L}P - \omega Q + \frac{3}{2L}(u_P - V_g^2),\\ \frac{dQ}{dt} &= \omega P - \frac{R}{L}Q - \frac{3}{2L}u_Q.\end{aligned} \tag{9}$$

Notice that, (9) is changed into a simple MIMO system with the coupling states.

C. Tracking Control Design

In this subsection, a new controller is designed to let the active and reactive powers track their references. Define errors of the active and reactive powers as follows:

$$\begin{aligned}e_P &:= P_{ref} - P,\\ e_Q &:= Q_{ref} - Q,\end{aligned} \tag{10}$$

where P_{ref} and Q_{ref} are the active and reactive power references, respectively. Consider the new MIMO system (9), it still has decoupling terms. Taking a control law with a feedforward and feedback such as

$$\begin{aligned}u_P &= \underbrace{V_g^2 + \frac{2R}{3}P + \frac{2L\omega}{3}Q}_{feedforward} + \frac{2L}{3}\nu_P,\\ u_Q &= \underbrace{\frac{2L\omega}{3}P - \frac{2R}{3}Q}_{feedforward} - \frac{2L}{3}\nu_Q,\end{aligned} \tag{11}$$

where ν_P and ν_Q are the feedback control inputs. If the feedback control inputs are designed as follows:

$$\begin{aligned}\nu_P &= \dot{P}_{ref} + K_{P,p}e_P + K_{P,i}\int_0^t e_P(\tau)d\tau,\\ \nu_Q &= \dot{Q}_{ref} + K_{Q,p}e_Q + K_{Q,i}\int_0^t e_Q(\tau)d\tau,\end{aligned} \tag{12}$$

where $K_{P,p}$, $K_{P,i}$, $K_{Q,p}$, and $K_{Q,i}$ are controller gains. Then, substituting (11) and (12) into (9), the error dynamics is obtained as follows:

$$\begin{aligned}\dot{P}_{ref} - \dot{P} = \dot{e}_P &= -K_{P,p}e_P - K_{P,i}\int_0^t e_P(\tau)d\tau,\\ \dot{Q}_{ref} - \dot{Q} = \dot{e}_Q &= -K_{Q,p}e_Q - K_{Q,i}\int_0^t e_Q(\tau)d\tau.\end{aligned} \tag{13}$$

If we define $\dot{\psi}_P = e_P$ and $\dot{\psi}_Q = e_Q$, the error dynamics (13) can be represented as follows:

$$\underbrace{\begin{bmatrix}\dot{e}_P\\ \dot{\psi}_P\\ \dot{e}_Q\\ \dot{\psi}_Q\end{bmatrix}}_{\dot{x}} = \underbrace{\begin{bmatrix}-K_{P,p} & -K_{P,i} & 0 & 0\\ 1 & 0 & 0 & 0\\ 0 & 0 & -K_{Q,p} & -K_{Q,i}\\ 0 & 0 & 1 & 0\end{bmatrix}}_{A}\underbrace{\begin{bmatrix}e_P\\ \psi_P\\ e_Q\\ \psi_Q\end{bmatrix}}_{x}. \tag{14}$$

If $K_{P,p}$, $K_{P,i}$, $K_{Q,p}$, and $K_{Q,i}$ are taken as positive values, then A has all negative eigenvalues. In other words, the closed-loop system is globally exponentially stable. Consequently, the controller gains could be designed by considering the damping ratio and settling time. Finally, based on (8), the original control inputs can be calculated as follows:

$$u_\alpha = \frac{v_{g\alpha}u_P - v_{g\beta}u_Q}{V_g^2}, \quad u_\beta = \frac{v_{g\beta}u_P + v_{g\alpha}u_Q}{V_g^2}. \tag{15}$$

Based on the proposed method, the system is changed into an LTI MIMO system. Fig. 2 shows the control inputs of the proposed method when active power is 1 kW and reactive power is 1 kVar. For the system (9), the control inputs u_P and u_Q are generated as constants, which means the proposed method has a similar construction to the conventional voltage-oriented control for VSCs. Consequently, the GVM-DPC makes a bridge between the DPC method and the conventional voltage-oriented control. In this paper, we only design the conventional control algorithm consisting of feedforward and PI feedback. However, various control methods based on the GVM-DPC could be designed for (9) to overcome appropriate issues.

D. Robust Control Design

In the practical operation, (14) could not be affected by the parameter uncertainties, discretization errors or measurement noises, etc.

Assumption 1: Consider the LTI MIMO system (9), suppose that there exist uncertainties δ_P, δ_Q, and Δ such that

$$\begin{aligned}\dot{x} &= f_a(x, u_P.u_Q, \delta_P, \delta_Q)\\ &= \begin{bmatrix}-\frac{R}{L}x_1 - \omega x_2 + \frac{3}{2L}(u_P - V_g^2) + \delta_P\\ \omega x_1 - \frac{R}{L}x_2 + \frac{3}{2L}u_Q + \delta_Q\end{bmatrix},\end{aligned} \tag{16}$$

This article has been accepted for publication in a future issue of this journal, but has not been fully edited. Content may change prior to final publication. Citation information: DOI 10.1109/TIE.2018.2801835, IEEE Transactions on Industrial Electronics

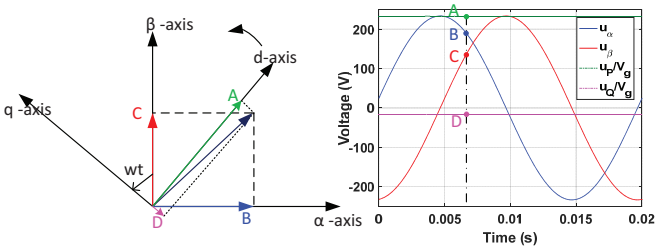

Fig. 2. Relationship between GVM-DPC and conventional DPC.

where δ_P and δ_Q are bounded such as

$$0 \leq |\delta_P| \leq \Delta, \quad 0 \leq |\delta_Q| \leq \Delta.$$

In VSC systems, a parameter uncertainty depends on the inductance, frequency or grid voltage. Of course, given an operating point, we need to estimate the upper bound of uncertainty, Δ. It is obvious that the regulation with the control law (11) with (12) always guarantees the exponential stability of the operating point for the nominal plant. The integral action compensates any DC offset due to model parameter uncertainty Furthermore, small perturbation from the equilibrium point is ultimately bounded by the exponential stability. Thus, Assumption 1 is reasonable without loss of generality.

Proposition 1: Consider the new MIMO system (9). If we take a control law such as

$$\begin{aligned}\hat{\nu}_P =& \dot{P}_{ref} + K_{P,p} e_P + K_{P,i} \int_0^t e_P(\tau) d\tau + K_P \mathrm{sgn}(e_P), \\ \hat{\nu}_Q =& \dot{Q}_{ref} + K_{Q,p} e_Q + K_{Q,i} \int_0^t e_Q(\tau) d\tau + K_Q \mathrm{sgn}(e_Q),\end{aligned} \tag{17}$$

where $K_P > \Delta$ and $K_Q > \Delta$, then the closed-loop system is also exponentially stable.

Proof: When $\delta_P = 0$ and $\delta_Q = 0$, the closed-loop system is exponentially stable based on (14). When $\delta_P \neq 0$ or $\delta_Q \neq 0$, we just consider δ_P and δ_Q terms for simplicity. Consider a Lyapunov function candidate such as

$$V = \frac{1}{2} e_P^2 + \frac{1}{2} e_Q^2. \tag{18}$$

The time derivative of (18) could be obtained as follows:

$$\dot{V} = e_P(\delta_P - K_P \mathrm{sgn}(e_P)) + e_Q(\delta_Q - K_Q \mathrm{sgn}(e_Q)). \tag{19}$$

If the controller gains are taken as $K_P > \Delta$ and $K_Q > \Delta$, then

$$\dot{V} \leq -K_{\Delta P}|e_P| - K_{\Delta Q}|e_Q|, \tag{20}$$

where $K_{\Delta P} = K_P - \Delta$ and $K_{\Delta Q} = K_Q - \Delta$.

Fig. 3 shows the block diagram of the proposed method. Notice that the proposed method presents the dynamics in d–q frame without PLL.

TABLE I
SYSTEM PARAMETERS USED IN SIMULATION AND EXPERIMENT

Parameter	Value	Unit
DC-link voltage	250	V
Line to line voltage(rms)	133	V
$R_{a,b,c}$	0.12	Ω
$L_{a,b,c}$	38	mH
AC frequency	50	Hz
Switching frequency	10	kHz

III. Simulation Results

The performance of the proposed method is verified by using a MATLAB/Simulink and PLECS environment. The topological model of the VSC is built by using the PLECS library, and the controller is implemented by using MATLAB/Simulink. The transient and steady-state performance of the GVM-DPC is compared with that of the PCH-DPC designed in [24] and the SMC-DPC designed in [20], which shows a better performance than the conventional DPC and the classical vector control designed in d-q frame. The parameters of the system used in the simulation and the experiment are described in Table I.

Fig. 4 describes the tracking performance of active and reactive powers, when the active power is stepped up from 0 to 1 kW at 0.02s and then back to 0 at 0.06s, and the reactive power is stepped up from 0 to 1 kVar at 0.04s and then back to 0 at 0.08s. By comparing with the active and reactive powers tracking performance of the PCH-DPC and the SMC-DPC, the GVM-DPC has significantly reduced ripples both in active and reactive powers. Moreover, the GVM-DPC has a faster tracking performance in active powers and a smaller overshoot in reactive power than those with the PCH-DPC and SMC-DPC. Unlike to the PCH-DPC and SMC-DPC, the proposed method has no need for consideration about switching delay or harmonics, and consequently, there are no difficult deciding boundary layer values. In addition, the proposed method gets the decoupled error dynamics of active and reactive powers which are globally exponentially stable. These features are similar with those designed in the d-q frame. As shown in Figs. 4(b), (d), and (f), it is clear that the output currents also have significantly reduced ripples in the proposed method.

The main disadvantage of DPC method is the steady-state performance (i.e. power ripple) compared to the methods designed in d-q frame. However, the proposed method overcomes that problem because it obtains a decoupled LTI error dynamics which is proven globally exponentially stable, which is the same as the methods designed in d-q frame. To validate this property, we set the active and reactive powers as 2 kW and 1 kVar, respectively. Fig. 5 shows the comparison of the harmonic performances of the output currents from 3rd to 49th harmonics. The GVM-DPC with sinusoidal PWM has the current THD of 1.4% which is less than 5% as commonly required for grid operation [39], which is hardly achieved in the PCH-DPC (THD=5.6%) and SMC-DPC (THD=6.0%). Therefore, the proposed GVM-DPC improves the harmonic spectrum of the output current without loss of transient response.

This article has been accepted for publication in a future issue of this journal, but has not been fully edited. Content may change prior to final publication. Citation information: DOI 10.1109/TIE.2018.2801835, IEEE Transactions on Industrial Electronics

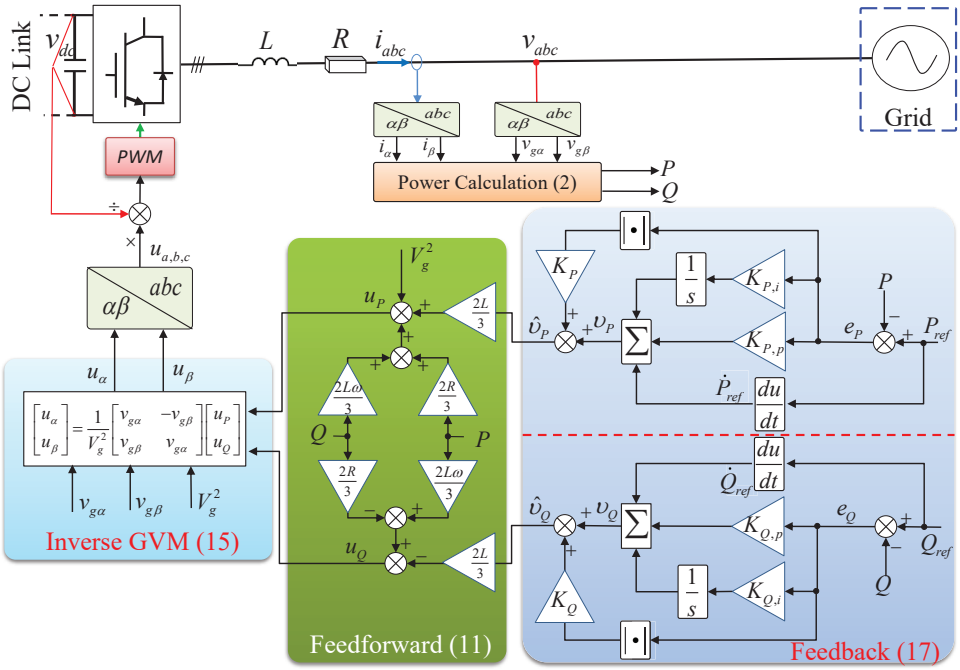

Fig. 3. Controller block diagram of the proposed GVM-DPC.

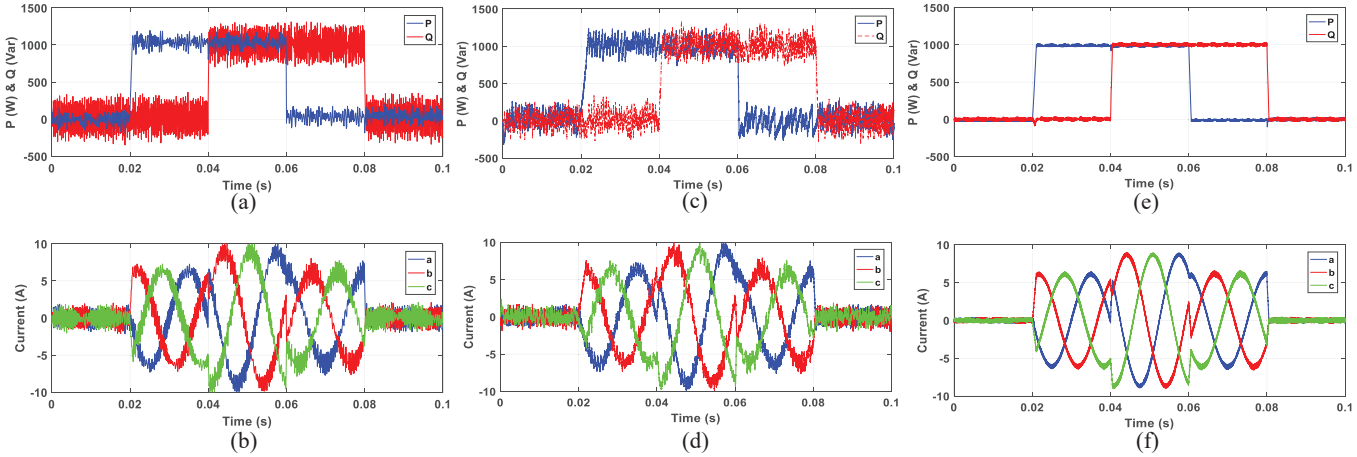

Fig. 4. Performance of the SMC-DPC: (a) active and reactive powers, (b) output currents; the PCH-DPC: (c) active and reactive powers, (d) output currents; the GVM-DPC: (e) active and reactive powers, (f) output currents.

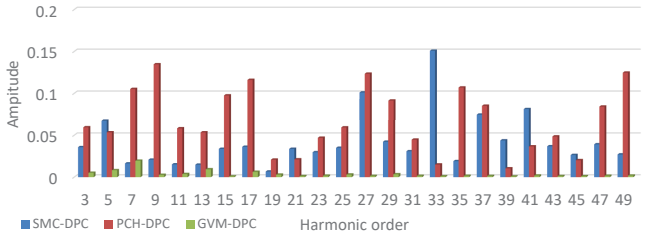

Fig. 5. Comparison of harmonic contents with the SMC-DPC, PCH-DPC, and GVM-DPC methods.

In order to test the feasibility of the proposed method in the low switching frequency application, we set the switching frequency of the VSC to 2 kHz. From Fig. 6, we can observe that the active power tracking performance of the proposed method with 2 kHz switching frequency. It is shown that the proposed method does not lose the feasibility.

IV. Experimental Results

The performance of the GVM-DPC method is also validated by using a Danfoss inverter (three-leg three-phase 2.2-kVA inverter with an L filter) and grid simulator, as shown in Fig. 7. The proposed control algorithm is developed in MATLAB/Simulink and compiled to dSPACE1006 system to switch the VSC. The switching frequency of the VSC is set to 10 kHz. The VSC is connected to the grid simulator, which emulates variable grid conditions.

This article has been accepted for publication in a future issue of this journal, but has not been fully edited. Content may change prior to final publication. Citation information: DOI 10.1109/TIE.2018.2801835, IEEE Transactions on Industrial Electronics

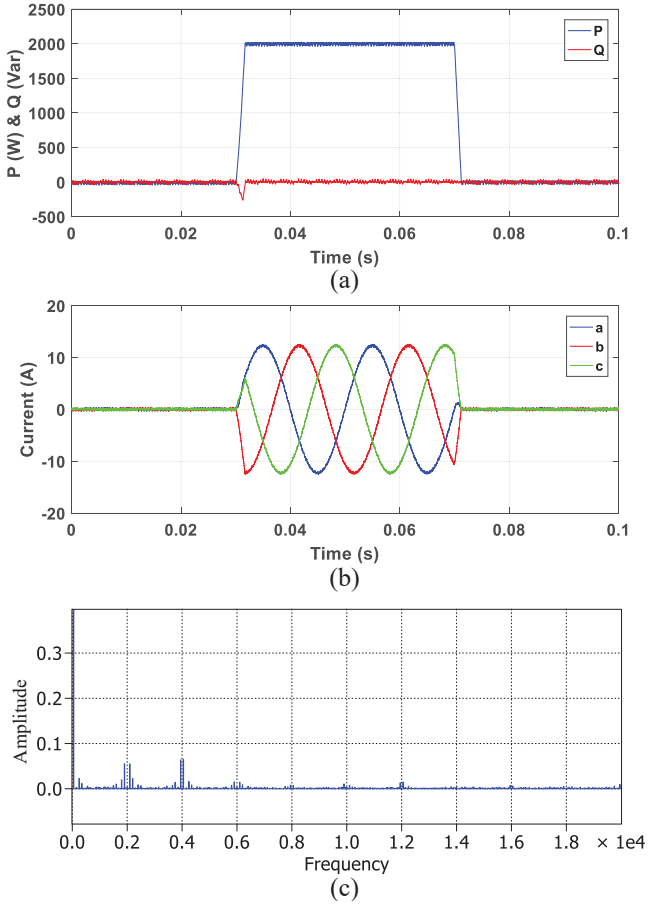

Fig. 6. Tracking performance of the GVM-DPC with 2kHz switching frequency: (a) active and reactive powers, (b) output currents, (c) current harmonic spectra.

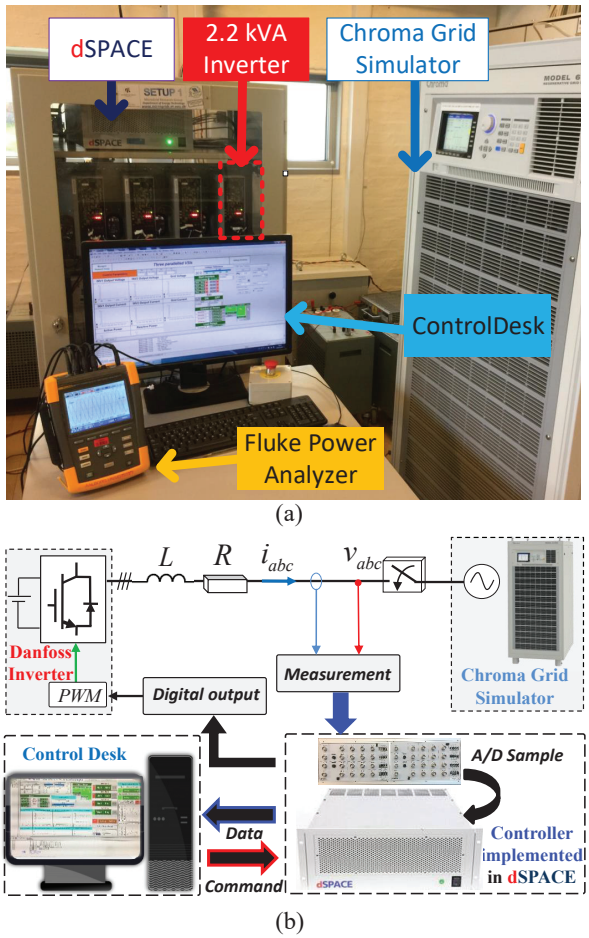

Fig. 7. (a) Experimental setup in the laboratory, (b) generic system architecture.

A. Tracking performance

The first test starts with the active power reference changing from 0 to 1 kW and maintaining and being back to 0, as shown in Fig. 8. In Fig. 8(a), the GVM-DPC has a fast transient response in active power tracking performance with a small overshoot. Fig. 8(b) shows the reactive power has a small overshoot but smoothly converges to its reference value. Fig. 9 shows the transient response using the GVM-DPC when the reactive power reference changes from 0 to 1 kVar and maintains 0.3s and goes back to 0. In this case, the GVM-DPC also has a fast transient response as well as low active and reactive power ripples.

B. Steady-state performance

The THD of the measured grid currents is illustrated when active power is 1 kW and reactive power is 1 kVar, as shown in Fig. 10. The THD of the output currents is measured as 1.9% by using the power analyzer, which is much less than the required THD value for grid operation.

C. Robustness performance

To validate the robust property, a low voltage ride through performance of proposed control technique is demonstrated in Fig. 11. A 10% voltage sag suddenly produced at 1.1s when the system injects 1 kW active power into the grid simulator and regulates 0 Var reactive power. The active power has a small overshoot (less than 10%) and converges to 1 kW, and the reactive power regulates 0 without overshoot, as shown in Figs. 11(a) and 11(b). Furthermore, the control performance is compared to the presence of line inductance variation. The line inductance in the control algorithm is set to 75% of the original value. The performance is similar to that without the line inductance variation. In addition, we insert 0.7% 5^{th} and 0.7% 7^{th} harmonics by using the grid simulator. The THD of the output currents is slightly increased to 2.4% when the THD of the grid voltage is 1.0%, as shown in Fig. 13. It still satisfies the requirements of grid operation. We also test active power tracking performance when the grid voltage has 5^{th} and 7^{th} harmonics. From Fig. 14, the tracking performance is not deteriorated. Finally, we test the robustness property to the grid frequency. The grid frequency is suddenly decreased from 50 Hz to 49.8 Hz by using the grid simulator, as shown in Fig. 15(a), while active and reactive powers are regulating 1 kW and 0 Var, respectively. The performance of active and reactive powers does not affect by the grid frequency deviation as well as the output currents, as shown in Figs. 15(b), (c), and (d). Consequently, we can conclude the proposed GVM-DPC

This article has been accepted for publication in a future issue of this journal, but has not been fully edited. Content may change prior to final publication. Citation information: DOI 10.1109/TIE.2018.2801835, IEEE Transactions on Industrial Electronics

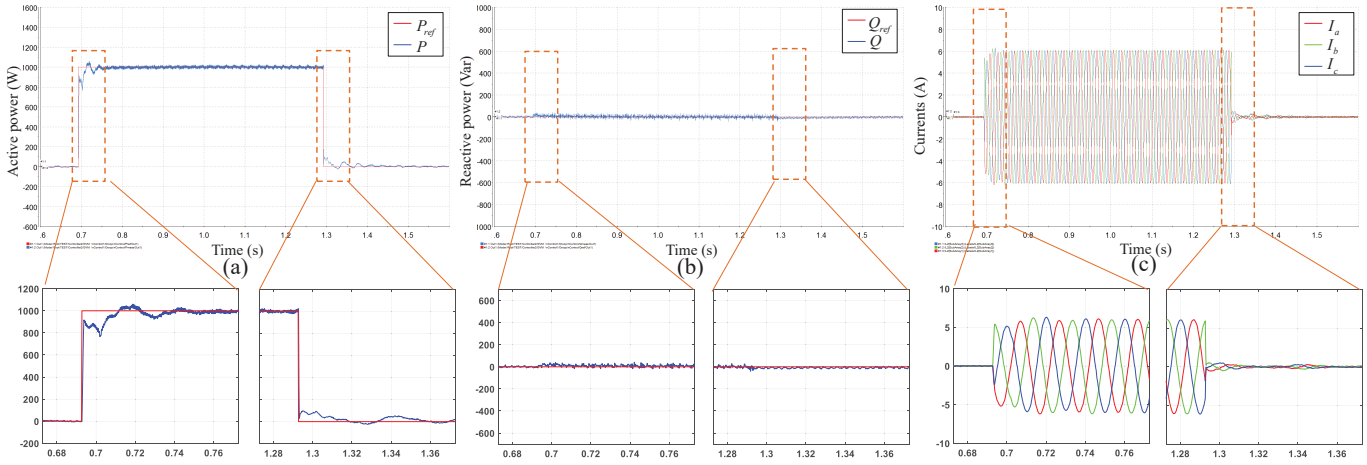

Fig. 8. Tracking behavior of the GVM-DPC (a) active power, (b) reactive power, (c) output currents, when $Q = 0$ Var and active power changes.

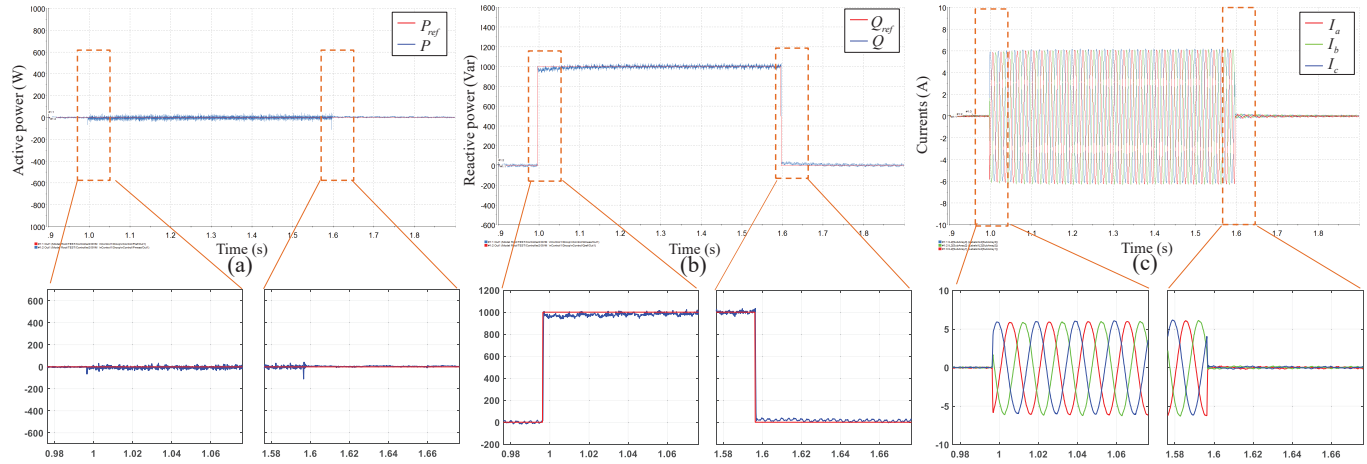

Fig. 9. Tracking behavior of the GVM-DPC (a) active power, (b) reactive power, (c) output currents, when $P = 0$ W and reactive power changes.

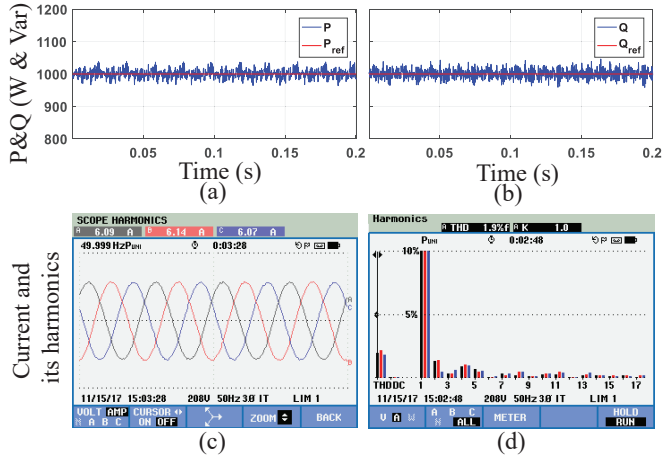

Fig. 10. Steady-state performance of the GVM-DPC with $P = 1$ kW and $Q = 1$ kVar. (THD=1.9%) (a) active power, (b) reactive power, (c) output currents, (d) currents spectrum.

has a robust property.

V. Conclusions

In this paper, we introduced an improved DPC control architecture called GVM-DPC for grid-connected VSC to control the instantaneous active and reactive powers directly. The GVM-DPC obtains not only the fast convergence of the instantaneous active and reactive powers but also the improved steady-state performance. Furthermore, the closed-loop system is exponentially stable in the whole operating range with the GVM-DPC. The proposed method was verified based on MATLAB/Simulink with PLECS. The simulation results showed that the proposed method has significantly reduced ripples both in active and reactive powers compared with the PCH-DPC and SMC-DPC. The THD of the output currents using the GVM-DPC is much less than 5% the requirement of the grid operator. Finally, the experimental results were provided and compared with the simulation results. Moreover, the robustness to the grid voltage and the line impedance was tested and the GVM-DPC has a robust property to such

This article has been accepted for publication in a future issue of this journal, but has not been fully edited. Content may change prior to final publication. Citation information: DOI 10.1109/TIE.2018.2801835, IEEE Transactions on Industrial Electronics

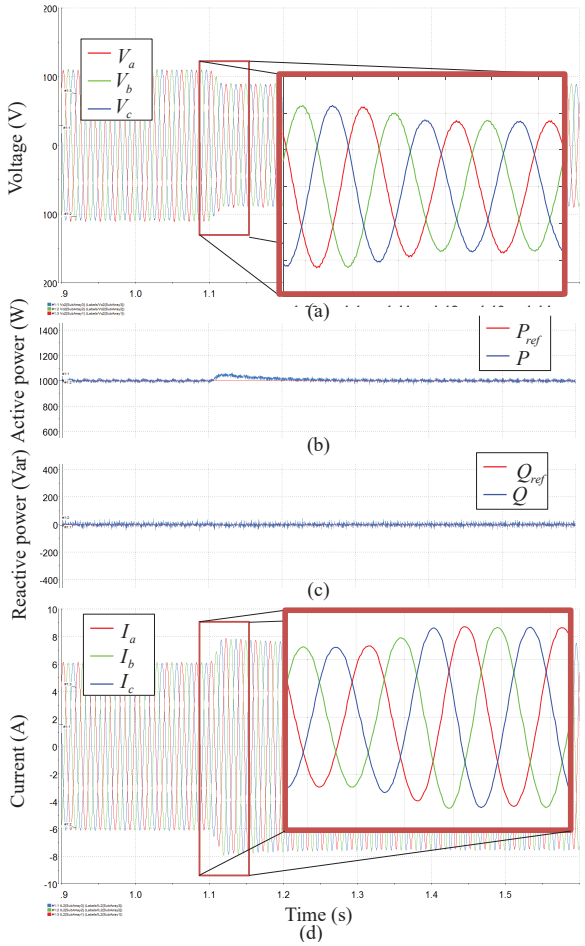

Fig. 11. Low voltage ride through performance of the GVM-DPC with active power being 1 kW and reactive power being 0 Var. (a) active power, (b) reactive power, (c) output currents.

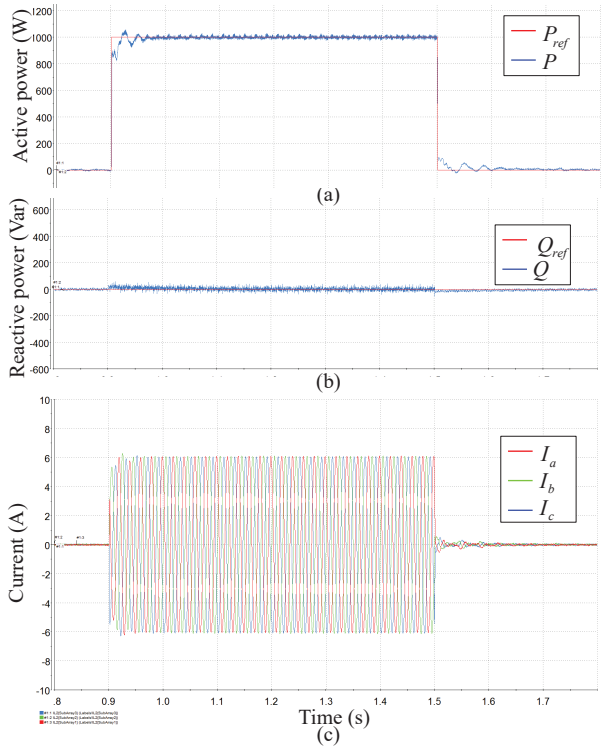

Fig. 12. Robustness performance of the GVM-DPC against the line inductances. (a) active power, (b) reactive power, (c) output currents.

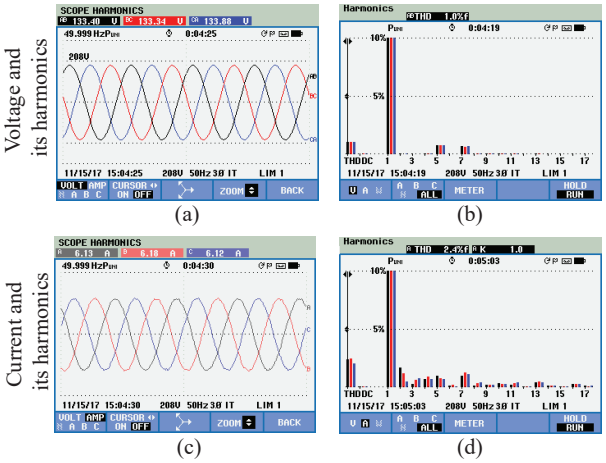

Fig. 13. Steady-state performance of the GVM-DPC with $P = 1$ kW and $Q = 1$ kVar. (a) grid voltages, (b) voltages spectrum (THD=1.0%), (c) output currents, (d) currents spectrum (THD=2.4%).

uncertainties. In the future work, the low switching frequency application and unbalanced systems will be further studied.

ACKNOWLEDGMENT

Y. Gui thanks Mr. Gibran Agundis-Tinajero (former Ph.D. Guest at AAU) for his help on the experimental setup.

REFERENCES

[1] Z. Chen, J. M. Guerrero, and F. Blaabjerg, "A review of the state of the art of power electronics for wind turbines," *IEEE Trans. Power Electron.*, vol. 24, no. 8, pp. 1859–1875, 2009.

[2] R. Teodorescu, M. Liserre, and P. Rodriguez, *Grid converters for photovoltaic and wind power systems*, vol. 29. John Wiley & Sons, 2011.

[3] F. Blaabjerg, M. Liserre, and K. Ma, "Power electronics converters for wind turbine systems," *IEEE Trans. Ind. Appl.*, vol. 48, no. 2, pp. 708–719, 2012.

[4] J. Rocabert, A. Luna, F. Blaabjerg, and P. Rodriguez, "Control of power converters in AC microgrids," *IEEE Trans. Power Electron.*, vol. 27, no. 11, pp. 4734–4749, 2012.

[5] J. C. Vasquez, J. M. Guerrero, M. Savaghebi, J. Eloy-Garcia, and R. Teodorescu, "Modeling, analysis, and design of stationary-reference-frame droop-controlled parallel three-phase voltage source inverters," *IEEE Trans. Ind. Electron.*, vol. 60, no. 4, pp. 1271–1280, 2013.

[6] Y. Gui, W. Kim, and C. C. Chung, "Passivity-based control with nonlinear damping for type 2 STATCOM systems," *IEEE Trans. Power Syst.*, vol. 31, no. 4, pp. 2824–2833, 2016.

[7] J. Jia, G. Yang, and A. H. Nielsen, "A review on grid-connected converter control for short circuit power provision under grid unbalanced faults," *IEEE Trans. Power Del.*, vol. PP, no. 99, pp. 1–1, 2017.

[8] Q.-C. Zhong, "Power-electronics-enabled autonomous power systems: Architecture and technical routes," *IEEE Trans. Ind. Electron.*, vol. 64, no. 7, pp. 5907–5918, 2017.

[9] N. Mohan, *Power electronics: a first course*. Wiley, 2011.

[10] R. Xu, Y. Yu, R. Yang, G. Wang, D. Xu, B. Li, and S. Sui, "A novel control method for transformerless H-bridge cascaded STATCOM with star configuration," *IEEE Trans. Power Electron.*, vol. 30, no. 3, pp. 1189–1202, 2015.

[11] Y. Wang, B. Ren, and Q.-C. Zhong, "Robust power flow control of grid-connected inverters," *IEEE Trans. Ind. Electron.*, vol. 63, no. 11, pp. 6887–6897, 2016.

[12] Z. Li, C. Zang, P. Zeng, H. Yu, S. Li, and J. Bian, "Control of a grid-

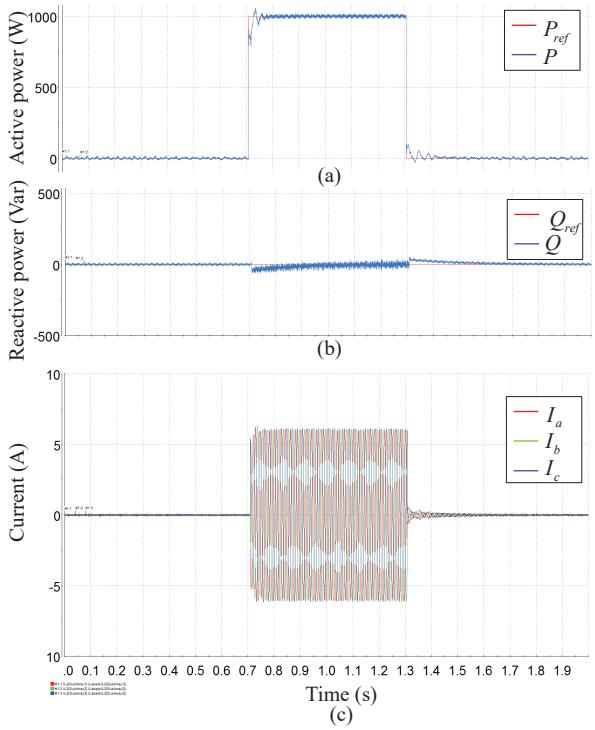

Fig. 14. Active power tracking behavior of the GVM-DPC (a) active power, (b) reactive power, (c) output currents, when the THD of voltage is 1.0%.

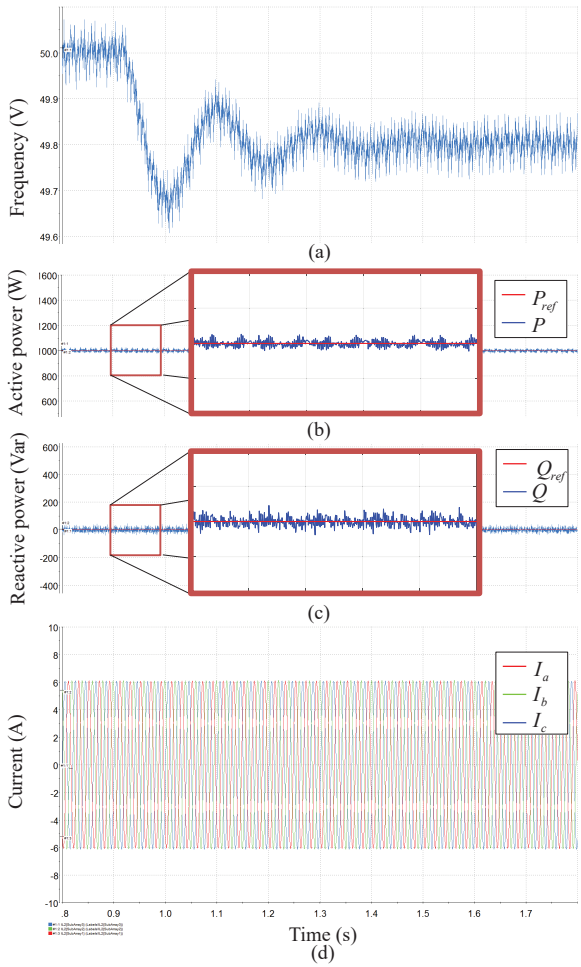

Fig. 15. Robustness performance of the GVM-DPC against the frequency. (a) Frequency of voltage, (b) active power, (c) reactive power, (d) output currents.

forming inverter based on sliding-mode and mixed H_2/H_∞ control," *IEEE Trans. Ind. Electron.*, vol. 64, no. 5, pp. 3862–3872, 2017.

[13] A. Abdelhakim, P. Mattavelli, P. Davari, and F. Blaabjerg, "Performance evaluation of the single-phase split-source inverter using an alternative DC-AC configuration," *IEEE Trans. Ind. Electron.*, vol. 65, no. 1, pp. 363–373, 2018.

[14] M. Kazmierkowski and L. Malesani, "Current control techniques for three-phase voltage-source PWM converters: a survey," *IEEE Trans. Ind. Electron.*, vol. 45, no. 5, pp. 691–703, Oct. 1998.

[15] M. Reyes, P. Rodriguez, S. Vazquez, A. Luna, R. Teodorescu, and J. M. Carrasco, "Enhanced decoupled double synchronous reference frame current controller for unbalanced grid-voltage conditions," *IEEE Trans. Power Electron.*, vol. 27, no. 9, pp. 3934–3943, 2012.

[16] T. Noguchi, H. Tomiki, S. Kondo, and I. Takahashi, "Direct power control of PWM converter without power-source voltage sensors," *IEEE Trans. Ind. Appl.*, vol. 34, no. 3, pp. 473–479, 1998.

[17] M. Malinowski, M. Jasiński, and M. P. Kazmierkowski, "Simple direct power control of three-phase PWM rectifier using space-vector modulation (DPC-SVM)," *IEEE Trans. Ind. Electron.*, vol. 51, no. 2, pp. 447–454, 2004.

[18] D. Zhi, L. Xu, and B. W. Williams, "Improved direct power control of grid-connected DC/AC converters," *IEEE Trans. Power Electron.*, vol. 24, no. 5, pp. 1280–1292, 2009.

[19] A. Bouafia, J.-P. Gaubert, and F. Krim, "Predictive direct power control of three-phase pulsewidth modulation (PWM) rectifier using space-vector modulation (SVM)," *IEEE Trans. Power Electron.*, vol. 25, no. 1, pp. 228–236, 2010.

[20] J. Hu, L. Shang, Y. He, and Z. Zhu, "Direct active and reactive power regulation of grid-connected DC/AC converters using sliding mode control approach," *IEEE Trans. Power Electron.*, vol. 26, no. 1, pp. 210–222, 2011.

[21] L. Shang and J. Hu, "Sliding-mode-based direct power control of grid-connected wind-turbine-driven doubly fed induction generators under unbalanced grid voltage conditions," *IEEE Trans. Energy Convers.*, vol. 27, no. 2, pp. 362–373, 2012.

[22] J. Hu and Z. Zhu, "Investigation on switching patterns of direct power control strategies for grid-connected DC–AC converters based on power variation rates," *IEEE Trans. Power Electron*, vol. 26, no. 12, pp. 3582–3598, 2011.

[23] S. S. Lee and Y. E. Heng, "Table-based DPC for grid connected VSC under unbalanced and distorted grid voltages: Review and optimal method," *Renew. Sustain. Energy Rev.,*, vol. 76, pp. 51–61, 2017.

[24] Y. Gui, G. H. Lee, C. Kim, and C. C. Chung, "Direct power control of grid connected voltage source inverters using port-controlled Hamiltonian system," *Int. J. Control Autom. Syst.*, vol. 15, no. 5, pp. 2053–2062, 2017.

[25] J. Rodriguez, M. P. Kazmierkowski, J. R. Espinoza, P. Zanchetta, H. Abu-Rub, H. A. Young, and C. A. Rojas, "State of the art of finite control set model predictive control in power electronics," *IEEE Trans. Ind. Informat.*, vol. 9, no. 2, pp. 1003–1016, 2013.

[26] S. Vazquez, J. I. Leon, L. G. Franquelo, J. Rodriguez, H. A. Young, A. Marquez, and P. Zanchetta, "Model predictive control: A review of its applications in power electronics," *IEEE Ind. Electron. Mag.*, vol. 8, no. 1, pp. 16–31, 2014.

[27] S. Kouro, M. A. Perez, J. Rodriguez, A. M. Llor, and H. A. Young, "Model predictive control: MPC's role in the evolution of power electronics," *IEEE Ind. Electron. Mag.*, vol. 9, no. 4, pp. 8–21, 2015.

[28] S. Vazquez, J. Rodriguez, M. Rivera, L. G. Franquelo, and M. Norambuena, "Model predictive control for power converters and drives: Advances and trends," *IEEE Trans. Ind. Electron.*, vol. 64, no. 2, pp. 935–947, 2017.

[29] S. Larrinaga, M. Vidal, E. Oyarbide, and J. Apraiz, "Predictive control strategy for DC/AC converters based on direct power control," *IEEE Trans. Ind. Electron.*, vol. 54, no. 3, pp. 1261–1271, 2007.

[30] P. Antoniewicz and M. P. Kazmierkowski, "Virtual-flux-based predictive direct power control of AC/DC converters with online inductance estimation," *IEEE Trans. Ind. Electron.*, vol. 55, no. 12, pp. 4381–4390, 2008.

[31] D.-K. Choi and K.-B. Lee, "Dynamic performance improvement of AC/DC converter using model predictive direct power control with finite control set," *IEEE Trans. Ind. Electron.*, vol. 62, no. 2, pp. 757–767, 2015.
[32] J. Hu, "Improved dead-beat predictive DPC strategy of grid-connected DC–AC converters with switching loss minimization and delay compensations," *IEEE Trans. Ind. Informat.*, vol. 9, no. 2, pp. 728–738, 2013.
[33] J. Hu and Z. Zhu, "Improved voltage-vector sequences on dead-beat predictive direct power control of reversible three-phase grid-connected voltage-source converters," *IEEE Trans. Power Electron.*, vol. 28, no. 1, pp. 254–267, 2013.
[34] Z. Song, W. Chen, and C. Xia, "Predictive direct power control for three-phase grid-connected converters without sector information and voltage vector selection," *IEEE Trans. Power Electron.*, vol. 29, no. 10, pp. 5518–5531, 2014.
[35] S. Vazquez, A. Marquez, R. Aguilera, D. Quevedo, J. I. Leon, and L. G. Franquelo, "Predictive optimal switching sequence direct power control for grid-connected power converters," *IEEE Trans. Ind. Electron.*, vol. 62, no. 4, pp. 2010–2020, 2015.
[36] J. Scoltock, T. Geyer, and U. K. Madawala, "Model predictive direct power control for grid-connected NPC converters," *IEEE Trans. Ind. Electron.*, vol. 62, no. 9, pp. 5319–5328, 2015.
[37] Y. Gui, C. Kim, and C. C. Chung, "Grid voltage modulated direct power control for grid connected voltage source inverters," in *Amer. Control Conf.*, pp. 2078–2084, 2017.
[38] F. Z. Peng and J.-S. Lai, "Generalized instantaneous reactive power theory for three-phase power systems," *IEEE Trans. Instrum. Meas.*, vol. 45, no. 1, pp. 293–297, 1996.
[39] "IEEE recommended practice and requirements for harmonic control in electric power systems," *IEEE Std 519-2014 (Revision of IEEE Std 519-1992)*, pp. 1–29, 2014.

Yonghao Gui (S'11-M'17) was born in Shenyang, China. He received the B.S. degree in automation from Northeastern University, Shenyang, China in 2009. He received the M.S. and Ph.D. degrees in electrical engineering from Hanyang University, Seoul, Korea in 2012 and 2017, respectively.

Since 2017, Dr. Gui has been working with the Department of Energy Technology, Aalborg University, Denmark, where he worked as a Postdoctoral Researcher at Microgrids Research Program (www.microgrids.et.aau.dk) from Feb. 2017 to Jan. 2018. His research interests include advanced control of power converter, microgrid, and renewable energy.

Chunghun Kim (S'12-M'18) received the B.S. degree in electronic electricity computer engineering from Hanyang University, Seoul, Korea, in 2011. He received the Ph.D. degree at the same university in 2018. He worked with National Renewable Energy Laboratory (NREL) as a visiting professional in 2017. His research interests include integration of renewable energy considering energy storage system control.

Chung Choo Chung (S'91-M'93) received his B.S. and M.S. degrees in electrical engineering from Seoul National University, Seoul, South Korea, and his Ph.D. degree in electrical and computer engineering from the University of Southern California, Los Angeles, CA, USA, in 1993. From 1994 to 1997, he was with the Samsung Advanced Institute of Technology, Korea. In 1997, he joined the Faculty of Hanyang University, Seoul, South Korea. He was an Associate Editor for the *Asian Journal of Control* from 2000 to 2002 and an Editor for the *International Journal of Control, Automation and Systems* from 2003 to 2005. He is currently An Associate Editor of journals including the IEEE TRANS. ON CONTROL SYSTEMS TECHNOLOGIES, IEEE TRANS. ON INTELLIGENT TRANSPORTATION SYSTEMS, and *IFAC Journal Mechatronics*. Dr. Chung is currently a general co-chair of IEEE CDC 2020, to be held in Korea. He is also 2018 President-elect of Institute of Control, Robotics and Systems, Korea.

Josep M. Guerrero (S'01-M'04-SM'08-FM'15) received the B.S. degree in telecommunications engineering, the M.S. degree in electronics engineering, and the Ph.D. degree in power electronics from the Technical University of Catalonia, Barcelona, in 1997, 2000 and 2003, respectively. Since 2011, he has been a Full Professor with the Department of Energy Technology, Aalborg University, Denmark, where he is responsible for the Microgrid Research Program (www.microgrids.et.aau.dk). His research interests is oriented to different microgrid aspects. As well, he received the best paper award of the Journal of Power Electronics in 2016. In 2014, 2015, 2016, and 2017 he was awarded by Thomson Reuters as Highly Cited Researcher, and in 2015 he was elevated as IEEE Fellow for his contributions on "distributed power systems and microgrids."

Yajuan Guan (S'12-M'16) received the B.S. degree and M.S. degree in electrical engineering from the Yanshan University, Qinhuangdao, Hebei, China, and the Ph.D. degree in power electronics from the Aalborg University, Aalborg, Denmark, in 2007, 2010 and 2016 respectively. From 2010 to 2012, she was an Assistant Professor in Institute of Electrical Engineering (IEE), Chinese Academy of Sciences (CAS). Since 2013, she has been a Lecturer in IEE; CAS. She is currently a Postdoctoral Fellow with Aalborg University, Aalborg, Denmark, as part of the Denmark Microgrids Research Programme (www.microgrids.et.aau.dk). Her research interests include microgrids, distributed generation systems, power converter for renewable energy generation systems, and energy internet.

Juan C. Vasquez (M'12-SM'14) received the B.S. degree in electronics engineering from UAM Manizales, Colombia, and the Ph.D. degree in automatic control, robotics, and computer vision from the Technical University of Catalonia, Barcelona, Spain, in 2004 and 2009, respectively. In 2011, He was Assistant Professor and from 2014 he is working as an Associate Professor at the Department of Energy Technology, Aalborg University, Denmark where he is the Vice Programme Leader of the Microgrids Research Program. His current research interests include operation, advanced hierarchical and cooperative control and the integration of Internet of Things into the SmartGrid. Dr. Vasquez is an Associate Editor of IET Power Electronics and in 2017 he was awarded by Thomson Reuters as Highly Cited Researcher.

Dr. Vasquez is currently a member of the IECSEG4 on LVDC Safety for use in Developed and Developing Economies, the TC-RES in IEEE Industrial Electronics, PELS, IAS, and PES Societies.